

Catalase Catalyses the Conversion of Ultraviolet-B Radiation Into Heat: Unexpected Role for Microorganisms in Sea Ice Melting and Sea Surface Warming

Cosme Marcos Moreno (✉ cosmemoreno1@gmail.com)

Hospital Universitario Torrecardenas <https://orcid.org/0000-0003-3944-279X>

Research Article

Keywords: Catalase, Hydrogen peroxide, UVB radiation, Photocatalytic thermogenesis, Ozone depletion, Sea ice meeting, Sea surface warming, Climate change

Posted Date: April 19th, 2021

DOI: <https://doi.org/10.21203/rs.3.rs-395188/v1>

License:   This work is licensed under a Creative Commons Attribution 4.0 International License.

[Read Full License](#)

Abstract

Catalase under ultraviolet-B radiation (CATUVB) produces reactive oxygen species (ROS), but the role of that surprising photoactivity in CAT still remains uncertain. On the other hand, it is well-known that CAT breaking down a steady source of hydrogen peroxide (H_2O_2) becomes inactive due to compound II formation (CII), which results in typical changes in its absorption spectrum. On the basis of CII formation, here I show first that CATUVB produces and breaks down H_2O_2 , via which UVB is converted into heat. I then show that CATUVB thermogenesis accelerates the ice melting and warms the medium. From data to nature, CAT converting harmful UVB into advantageous heat in microorganisms would be responsible for a hidden biogeochemical thermogenesis process under the ozone layer control with effects on sea ice melting and sea surface warming in cold regions.

Introduction

It is widely accepted that CAT breaks down H_2O_2 from cellular metabolism, but some believe the ultimate role of such a venerable enzyme may still be a mystery (Kirkman and Gaetani 2007). In support of this view, it was unexpectedly discovered that CAT is a photoactive enzyme, responsible for the production of ROS in cells exposed to UVB (Heck et al. 2003). UVB-driven photoactivity has so far been shown in CAT with bound NADPH (Kirkman and Gaetani 1984; Fita and Rossmann 1985) from mammals and bacteria (Heck et al. 2010). Regarding the ROS product, preliminary data excluding superoxide anion and singlet oxygen rather supported “peroxide” species, likely H_2O_2 (Heck et al. 2003, 2010). Whether or not CATUVB produces H_2O_2 remains unresolved, probably because H_2O_2 is the substrate of CAT, one of the fastest-acting enzymes in biology. So, with the lack of further data, the role of CATUVB still remains uncertain.

On the other hand, it has long been known that CAT exposed to a constant H_2O_2 source, as generated by the notatin system (NS) (i.e. glucose oxidase/glucose), becomes progressively inactivated due to CII formation (Chance 1950; Keilin and Nicholls 1958; Kirkman et al. 1987). CII formation during the CAT catalytic cycle can be summarized as follows: the resting CAT reacts with H_2O_2 yielding H_2O and compound I (CI), whose reaction with a second H_2O_2 yields O_2 , H_2O and the resting enzyme. However, when decomposing a steady source of H_2O_2 , CI is progressively one electron oxidized by an endogenous electron donor generating inactive CII, which causes a unique increase in absorption at 435 nm. Typically, CII formation is strongly accelerated by an exogenous electron donor, such as ferrocyanide, and reverses spontaneously (Chance 1950; Kirkman et al. 1987). Thus, if CII formation invariably occurs when CAT is exposed to a source of H_2O_2 , CII formation in CATUVB would be evidence for H_2O_2 photoproduction, which could pave the way to a better understanding of the role of CATUVB.

Material And Methods

Commercial crystallised CAT from beef liver (> 60.000 U.I./mg of protein) was from Worthington Biochemical Corporation. NADPH, 2'-7'-dichlorofluorescein diacetate (H2DCFDA), ferrocyanide and

dimethyl sulfoxide (DMSO) were from Sigma-Aldrich.

A UVB transilluminator CU10A (CLINX) with a maximal intensity of $800 \mu\text{W}/\text{cm}^2$ at 302 nm was used for irradiation. UVB intensity was measured by a radiometer UV340B (Sampometer). Temperature was measured by a Center 306 dual datalogger thermometer (Center Technology Corp.) with a resolution of 0.1°C , using K type beaded thermocouple probes (TP-K01). A UV-VIS 1200 spectrophotometer was used for all purposes.

CAT preparation

Crystallised CAT suspension in 0.1 % thymol was directly dissolved in 20 mM potassium phosphate buffer, pH 7.4, for 30' and centrifuged 10' at 10.000 rpm to remove any precipitate (Hillar and Nicholls 1992). CAT concentration was measured in terms of haematin content, considering an extinction coefficient of $120 \text{ mM}^{-1} \text{ cm}^{-1}$ at 405 nm (Hillar et al. 1994).

Irradiation procedure

Samples, usually of 1ml, inside quartz or polymethylmethacrylate (PMMA) cuvettes were irradiated in horizontal position from above. Only one light bar of the transilluminator was used, so cuvette and bar were aligned along their major axis. The desired UVB intensity was achieved with the transilluminator potentiometer or by placing the samples at a suitable distance from the transilluminator surface.

CII formation and NADPH oxidation measurement

CII formation by UVB irradiation was measured by the increase in absorbance at 435 nm, as previously described (Chance 1950, Kirkman et al. 1984). Kinetics of CII formation versus irradiation was carried out by irradiating one CAT sample and measuring the absorbance at given times. CII concentration was calculated considering an extinction coefficient of $32 \text{ mM}^{-1} \text{ cm}^{-1}$ (Chance 1950, Kirkman et al. 1984). NADPH oxidation was measured by the decrease in absorbance at 340 nm, considering an extinction coefficient for NADPH of $6,2 \cdot 10^3 \text{ M}^{-1} \text{ cm}^{-1}$.

ROS detection

ROS output by CAT_{UVB} was detected by 2'-7'-dichlorofluorescein diacetate (H2DCFDA) oxidation (Heck et al. 2003, Murakami et al. 2008) yielding 2'-7'-dichlorofluorescein (DCF), which was measured by the absorption increase at 504 nm (Valkonen et al. 1997, Murakami et al. 2008). 10 mM H2DCFDA was prepared in DMSO, and the concentration in samples was $25 \mu\text{M}$. In our experimental conditions, the oxidized H2DCFDA decomposes slowly into DCF, so absorbance at 504 nm was measured 24 hours after irradiation.

Observation of CATUVB thermogenesis

For the temperature-controlled UVB irradiation experiments, silicone-sealed PMMA cuvettes containing CAT and control samples were housed in cavities made of expanded polystyrene (EPS) modules, so that

only the surface to be irradiated was free of insulation. Special care was taken so that temperature changes were identical in both cuvettes in any condition, in particular under UVB irradiation given that the UVB-transilluminator is a significant heat source. Temperature was measured by a K type beaded thermocouple probe (TP-K01) with teflon tape insulation, inserted into the cuvette through the silicone stopper. For experiments at temperatures below 0° C, CAT and control samples were first frozen at -19° C and then allowed to melt spontaneously at room temperature of 13 °C, with UVB irradiation starting at -5°C. For experiments at temperatures up 0° C, CAT and control samples at room temperature of 13° C were irradiated until the temperature increased to 5° C (i.e. above 18° C).

Data processing

Data were processed with Graph Pad Prism. Unless stated differently, measurements were carried out in duplicate (mean \pm SD). Temperature charts were directly obtained by unloading logged temperature data into a PC interface with Windows software (SE 305, version 4.8.0.0). Schematic figures were carried out with Power Point from Microsoft.

Results And Discussion

CII formation by CATUVB

CATUVB experiences an immediate increase in absorption at 435 nm (Fig. 1aA). More importantly, this increase in absorption is strongly accelerated by ferrocyanide (Fig. 1aB). Moreover, consistent with CII formation, the increase in absorption is reversible upon cessation of UVB irradiation (Fig. 1a). UVB-driven CII formation is also evident in full CAT spectra (Chance 1950, Kirkman et al. 1987), especially in the presence of ferrocyanide, where most of the CAT is converted to CII (Fig. 1b). Consequently, UVB-driven CII formation shows that CATUVB produces and breaks down H_2O_2 .

CATUVB kinetics

CII formation is directly related to UVB intensity and CAT concentration, proceeding at a constant rate of 0.024 CII nmol/CAT_{heme} nmol/ml/min under UVB intensity of 450 $\mu W/cm^2$. As a comparison, CII generates at rate of 0.021 nmol/CAT_{heme} nmol/ml/min in the presence of NS producing 2 H_2O_2 nmol/ml/min (Kirkman et al. 1987). CII formation is initially linear, decreasing slowly to reach a plateau after 40' of UVB irradiation (Fig. 1 aA). Since CII decays spontaneously (Chance 1950; Kirkman et al. 1987), such a plateau represents a steady state where CII formation and decomposition occur at the same rate. Of note, CII formation and H_2O_2 production follow the same kinetics (Fig. 1c), which supports that H_2O_2 photoproduction is inhibited by inactive CII formation. A conformational mechanism could contribute to the link of H_2O_2 photoproduction and CII formation, as the latter's spectral change (Fig. 1b) must entail a conformational change in CAT. In summary, inactive CII formation due to H_2O_2 break down inhibits H_2O_2 photoproduction, which given the harmful nature of H_2O_2 would be essential to prevent CATUVB toxicity in cells.

The effect of NADPH on CATUVB

It has been exhaustively shown that NADPH (but not NADH) traces inhibit CII formation or accelerate its decay in CAT exposed to NS (Kirkman et al. 1987; Hillar and Nicholls 1992; Hillar et al. 1994), so it is believed that NADPH plays a physiological role in keeping CAT catalytic activity at H_2O_2 levels that occur naturally in cells. NADPH is oxidized in this process at rates that depend on the rate of H_2O_2 production by NS, both processes being not at all stoichiometric (Kirkman et al. 1987). NADPH is also oxidised by CATUVB at a constant rate of $0.13 \text{ NADPH nmol/CAT}_{\text{hem}} \text{ nmol/min}$ under UVB intensity of $450 \mu\text{W/cm}^2$. NADPH also decreases CII concentration at plateau in a concentration-dependent manner, which results in a similar decrease in H_2O_2 levels (Fig. 1d). Thus, NADPH inhibiting CII formation achieves a new steady state in which CATUVB produces and decomposes more H_2O_2 (Fig. 1d) in a way that CATUVB activity would naturally be driven by NADPH concentrations.

CATUVB thermodynamics

Now the question is: why does CATUVB generate H_2O_2 only then to break it down? In other words: what is CAT actually doing in cells under solar UVB? CATUVB uses O_2 and H_2O to produce H_2O_2 (Heck et al. 2003), which is then decomposed into H_2O and O_2 . That is, CATUVB performs a cyclic reaction that does not produce any chemical energy, so given that light emission (i.e. fluorescence) by CAT excited by UVB is negligible (Yekta et al. 2017), all UVB used for H_2O_2 synthesis finally becomes heat. Assuming that one H_2O_2 molecule is produced per UVB photon absorbed, the energy of one einstein of UVB photons at 300 nm ($E_{\text{mol}} = N h \nu$) being around 400 kJ would be the heat released per mol of H_2O_2 generated and decomposed by CATUVB.

The effect of CATUVB on the medium temperature

CATUVB releasing about 13 times the free energy of ATP hydrolysis (i.e. 30,5 kJ/mol) would be by far the most exothermic process in biology. Warm temperature is essential for sustaining life processes, so that powerful CATUVB thermogenesis would only make sense if CATUVB works in a cold environment. In fact, ROS output by CATUVB was observed to proceed at significant rate at 0 °C (Heck 2003). Accordingly, CATUVB could produce heat from UVB even at very low temperatures, which could be experimentally observed. Thus, in experimental conditions where CAT and control samples were first frozen between -19° and -15° C and then allowed to warm at room temperature of around 13°C, with UVB irradiation starting at -5°C (see Methods), data show a difference in temperature in CAT samples with regard to controls peaking at between -1,0 and 1,0 °C (Fig. 2a). So, CATUVB thermogenesis would be contributing to the specific heat of ice melting. Likewise, when irradiated at 13°C, the increase in temperature is faster in CAT samples than in controls, with a difference of around 0,2 – 0,3 °C at 20 minutes (Fig. 3b). Given the experimental conditions involving an irradiation surface of $1,2 \text{ cm}^2$, 0,8 ml of sample volume and CAT concentration enough as to absorb most UVB radiation at 300 nm, about 0.8 J would be needed for a such difference in temperature, which is consistent with the 0.86 J delivered in 20 minutes by the UVB-

transilluminator at an intensity of $600 \mu\text{W}/\text{cm}^2$. Ferrocyanide made possible the experimental observation of CATUVB thermogenesis, due to CATUVB producing more heat in its presence than alone or in the presence of NADPH.

The role of CATUVB: from data to nature

A) CATUVB and life evolution

It is well-known that UVB is harmful to cells and that most of the catalytic reactions that sustain life are cold-sensitive. However, life on Earth has evolved under extremely adverse cold and UVB conditions, most of the time acting together (Russell 1990; Kasting and Siefert 2002; Sinha and Häder 2002; McKencie et al. 2002; Karam 2003; Hessen 2008). Data have shown here that CAT converts UVB into heat at very low temperatures (Fig. 2), which reveals the role of CATUVB in nature. That is, CATUVB producing beneficial heat from harmful UVB, is responsible for an unprecedented thermogenesis that allows cells to evolve under adverse cold and UVB conditions (Fig. 3). In this regard, CAT is known to evolve in Precambrian eons, 3,5 Gy ago (Zámocký et al. 2012), precisely when microorganisms were subjected to high-intensity UVB due to the low levels of atmospheric O_2 (McKencie et al. 2002; Karam 2003) and an extremely cold climate (Kasting and Siefert 2002), including several low-latitude glaciations episodes known as Snowball Earth (Hoffman et al. 1998; Kirschvink et al. 2000;). Furthermore, evidence for H_2O_2 photoproduction during such cold periods supports CATUVB activity, whose thermogenesis might pave the way to the rise of oxygenic photosynthesis (McKay and Hartman 1991; Kasting and Siefert 2002; Liang et al. 2006). In turn, oxygenic photosynthesis being the main NADPH and O_2/O_3 producer would become the primary driver of CATUVB thermogenesis (Fig. 4).

B) CATUVB playing a biogeochemical process with impact on ice melting and sea warming

Thermogenesis due to an unknown UVB-driven H_2O_2 synthesis and its decomposition by CAT in microorganisms has been previously proposed as a photocatalytic factor in sea ice melting and sea warming in cold regions with severe ozone depletion (Moreno 2012). Experimental evidence for that UVB thermogenesis (Fig. 2) in microorganisms is now evidence for such a hypothesis. Vice versa, CATUVB activity in the enormous mass of microbes living in sea ice (SIMCO) (Palmisano and Sullivan 1983; Smith and Nelson 1986; Kottmeier and Sullivan 1988), sea ice edge (Smith and Nelson 1986; Russell 1990) and sea surface of cold regions (Behrenfeld et al. 2006; Sigman and Hain 2012) would be responsible for a process of biogeochemical thermogenesis under the ozone layer control with effects on ice melting and sea warming in cold regions.

Conclusions

Experimental evidence based on CII formation has shown that CATUVB produces and breaks down H_2O_2 , a highly regulated photocatalysis under control of NADPH whose ultimate effect is the transformation of

UVB into heat. Moreover, it is shown here that such UVB-driven thermogenesis accelerates ice melting and warms the medium. CATUVB would allow microorganisms to evolve in adverse cold and UVB conditions. Furthermore, that UVB-driven thermogenesis in the huge mass of microbes living in sea ice and sea surface would be responsible for a new ozone layer-driven biogeochemical process with effects on the biosphere evolution.

Declarations

Acknowledgements

I am very grateful to Stephen J. Malcolm from Cefas, UK, and Ignacio Fita Rodriguez from CSIC, Spain, for their helpful comments.

Author Contributions

Cosme M . Moreno is the only and corresponding author.

Funding

No funding was received for conducting this study.

Financial/non-financial interests

The author has no relevant financial or non-financial interests to disclose.

Data availability statement

The datasets generated during and/or analysed during the current study are available from the corresponding author on reasonable request.

References

1. Behrenfeld MJ, O'Malley RT, Siegel DA, McCain CR, Sarmiento JJ, Feldman GC, Milligan AJ, Falkowski PG, Letelier RM, Boss ES (2006) Climate-driven trends in contemporary ocean productivity. *Nature* 444:752-755. DOI: [10.1038/nature05317](https://doi.org/10.1038/nature05317)
2. Chance B. The reactions of catalase in the presence of the notatin system (1950) *Biochem J* 46:387-402. doi: [10.1042/bj0460387](https://doi.org/10.1042/bj0460387)
3. Fita I, Rossmann MG (1985) The NADPH binding site on beef liver catalase. *Proc Natl Acad Sci USA* 82:1604-1608.
4. Heck DE, Vetrano AM, Mariano TM, Lasking JD (2003) UVB lighth stimulates production of reactive oxygen species. Unexpected role for catalase. *J Biol Chem* 278:22432-22436. DOI: [10.1074/jbc.C300048200](https://doi.org/10.1074/jbc.C300048200)

5. Heck DE, Shakarjian M, Kim HD, Lasking JD, Vetrano AM (2010) Mechanism of oxidant generation by catalase. *Ann NY Acad Sci* 1203:120-125. DOI: [10.1111/j.1749-6632.2010.05603.x](https://doi.org/10.1111/j.1749-6632.2010.05603.x)
6. Hessen DO (2008) Solar radiation and life evolution. In: Bjertness E (ed) *Solar Radiation and Human Health*. The Norwegian Academy of Sciences and Letters, Oslo, pp 123-134.
7. Hillar A, Nicholls P (1992) A mechanism for NADPH inhibition of catalase compound II formation. *FEBS Lett* 314:179-182. DOI: [10.1016/0014-5793\(92\)80969-n](https://doi.org/10.1016/0014-5793(92)80969-n)
8. Hillar A, Nicholls P, Switala J, Loewen PC (1994) NADPH binding and control of catalase compound II formation: comparison of bovine, yeast and *Escherichia coli* enzymes. *Biochem J* 300:531-539. DOI: [10.1042/bj3000531](https://doi.org/10.1042/bj3000531)
9. Hoffman PF, Kaufman AJ, Halverson GP, Schrag DP (1998) A neoproterozoic snowball Earth. *Science* 281:1342-1346. DOI: [10.1126/science.281.5381.1342](https://doi.org/10.1126/science.281.5381.1342)
10. Karam PA (2003) Inconstant Sun: how solar evolution has affected cosmic and ultraviolet radiation exposure over the history of life on Earth. *Health Physics* 84:322-333. DOI: [10.1097/00004032-200303000-00005](https://doi.org/10.1097/00004032-200303000-00005)
11. Kasting JF, Siefert JL (2002) Life and the evolution of Earth's atmosphere. *Science* 296:1066-1068. DOI: [10.1126/science.1071184](https://doi.org/10.1126/science.1071184)
12. Keilin D, Nicholls P (1958) Reactions of catalase with hydrogen peroxide and hydrogen donors. *Biochim Biophys Acta* 29:302-307. <https://doi.org/10.1042/bj3000531>
13. Kirkman HN, Gaetani G F (1984) Catalase: a tetrameric enzyme with four tightly bound molecules of NADPH. *Proc Natl Acad Sci USA* 81:4343-4347. DOI: [10.1073/pnas.81.14.4343](https://doi.org/10.1073/pnas.81.14.4343)
14. Kirkman HN, Galiano S, Gaetani GF (1987) Function of catalase-bound NADPH. *J Biol Chem* 262:660-666.
15. Kirkman HN, Gaetani GF (2007) Mammalian catalase: a venerable enzyme with new mysteries. *Trends Biochem Sci* 32:44-50. <https://doi.org/10.1016/j.tibs.2006.11.003>
16. Kirschvink J L, Gaidos EJ, Bertani LE, Beukes NJ, Gutzmer N, Maepa LN, Steinberger RE (2000) Paleoproterozoic snowball Earth: Extreme climatic and geochemical global change and its biological consequences. *Proc Natl Acad Sci USA* 97:1400-1405. DOI: [10.1073/pnas.97.4.1400](https://doi.org/10.1073/pnas.97.4.1400)
17. Kottmeier ST, Sullivan CW (1988) Sea ice microbial communities (SIMCO). *Polar Biol* 8:293–304. <https://doi.org/10.1007/BF00263178>
18. Liang MC, Hartman H, Kopp RE, Kirschvink JL, Yung YL (2006) Production of hydrogen peroxide in the atmosphere of a Snowball Earth and the origin of oxygenic photosynthesis. *Proc Natl Acad Sci USA* 103:18896-18899. <https://doi.org/10.1073/pnas.0608839103>
19. Mckay CP, Hartman H (1991) Hydrogen peroxide and the evolution of oxygenic photosynthesis. *Orig Life Evol Biosph* 21:157-163. <https://doi.org/10.1007/BF01809444>
20. McKencie RL, Björn LO, Bais A, Ilyas M (2002) Changes in biologically active ultraviolet radiation reaching the Earth's surface. *Photochem Photobiol Sci* 2:5-15. <https://doi.org/10.1039/b211155c>

21. Moreno CM (2012). Hydrogen peroxide production driven by UVB in planktonic microorganisms: a photocatalytic factor in sea warming and ice melting in regions with ozone depletion? *Biogeochemistry* 107:1-8. <https://doi.org/10.1007/s10533-010-9566-7>
22. Murakami M, Taniguchi M, Takama M, Cui J, Oyanagui Y (2008) UVB-dependent generation of reactive oxygen species by catalase and IgG under UVB light: Inhibition by antioxidants and anti-inflammatory drugs. *Drug Discov Ther* 2:85-93.
23. Russell NJ (1990) Cold adaptation in microorganisms. *Phil Trans R Soc Lond B* 326:595-611. <https://www.jstor.org/stable/2398707>
24. Sigman DM, Hain MP (2012) The Biological Productivity of the Ocean. *Nature Education Knowledge* 3:1-16.
25. Sinha RP, Häder D-P (2002) Life under solar UV radiation in aquatic organisms. *Adv Space Res* 30:1547- 1556. [https://doi.10.1016/S0273-1177\(02\)00370-8](https://doi.10.1016/S0273-1177(02)00370-8)
26. Valkonen M, Kuusi T (1997) Spectrophotometric assay for total peroxyl radical-trapping antioxidant potential in human serum. *J Lipid Res* 38:823-833. [https://doi.10.1016.S0022-2275\(20\)37249-7](https://doi.10.1016.S0022-2275(20)37249-7)
27. Yekta R, Dehghan G, Rashtbari S, Sheibani N, Moosavi-Movahedi A (2017) Activation of catalase by pioglitazone: Multiple spectroscopic methods combined with molecular docking studies. *J Mol Recognit* 30, <https://doi.0.1002/jmr.2648>
28. Zámocký M, Gasselhuber B, Furtmüller PG, Obinger C (2012) Molecular evolution of hydrogen peroxide degrading enzymes. *Arch Biochem Biophys* 525:131-144. <https://doi.org/10.1016/j.abb.2012.01.017>

Figures

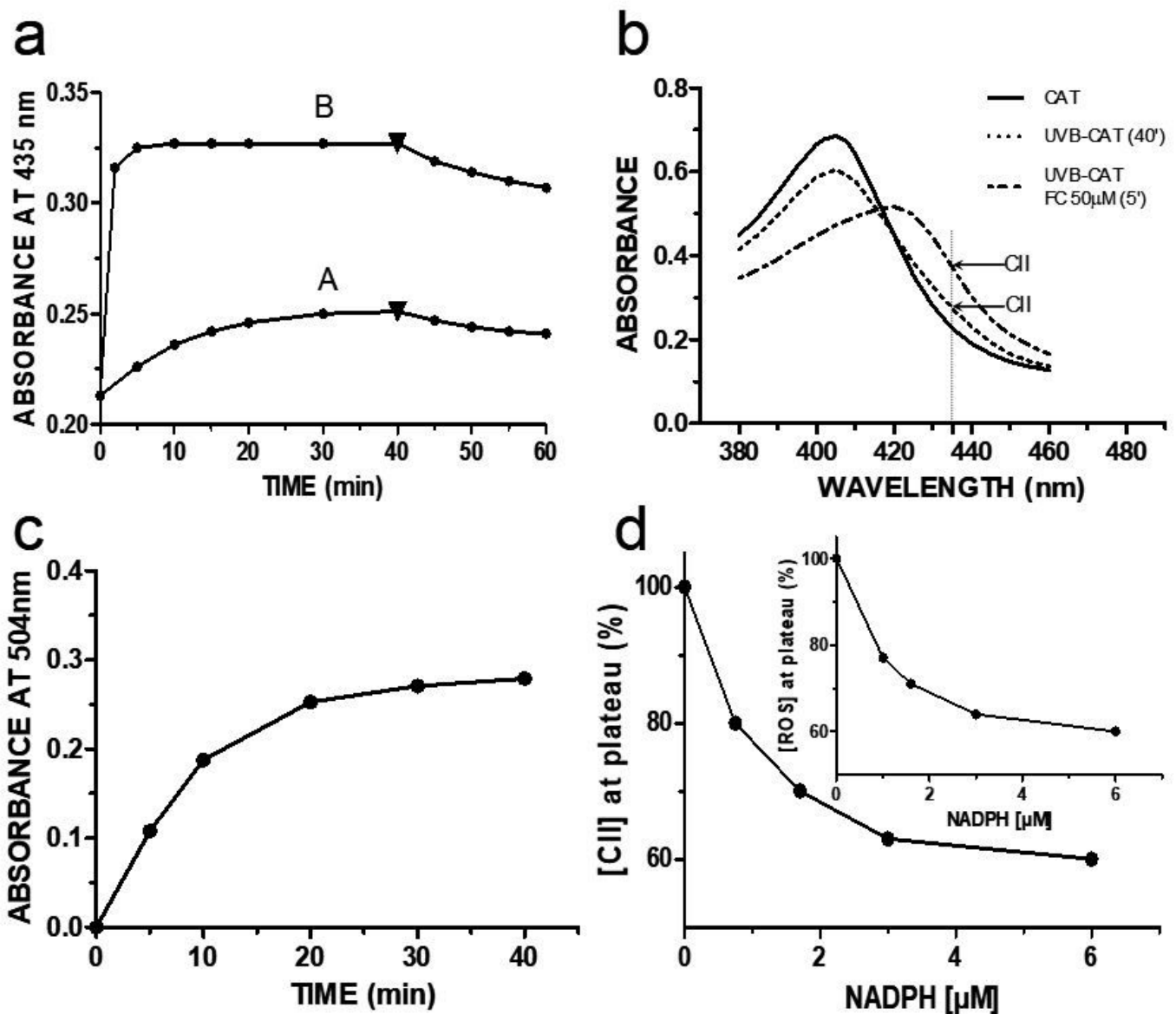


Figure 1

a) Absorption increase at 435 nm in CAT (4 μ M CATheme under UVB intensity of 450 mW/cm²) showing CII formation. A: CAT alone. B: in the presence of 50 μ M ferrocyanide. One sample was used for each curve. Arrow heads indicate end of UVB irradiation. b) CAT spectrum (5,7 μ M CATheme) from 380 to 460 nm and its spectral changes after 40 minutes of UVB irradiation, and in the presence of ferrocyanide (50 μ M) after 5 minutes. Arrows point to the absorbance increase at 435 nm (vertical line) showing CII formation. c) ROS/H₂O₂ production by CATUVB (1 μ M CATheme). Absorbance at 504 nm was measured 24 hours after irradiation. d) The effect of NADPH on CII formation by CATUVB (4 μ M CATheme under UVB intensity of 450 mW/cm²). CII formation at plateau was measured in CAT samples containing different NADPH concentrations. Inset: The effect of NADPH on ROS/H₂O₂ production by CATUVB (1 μ M CATheme). Same procedure as for CII formation. Absorbance at 504 nm was measured 24 hours after irradiation.

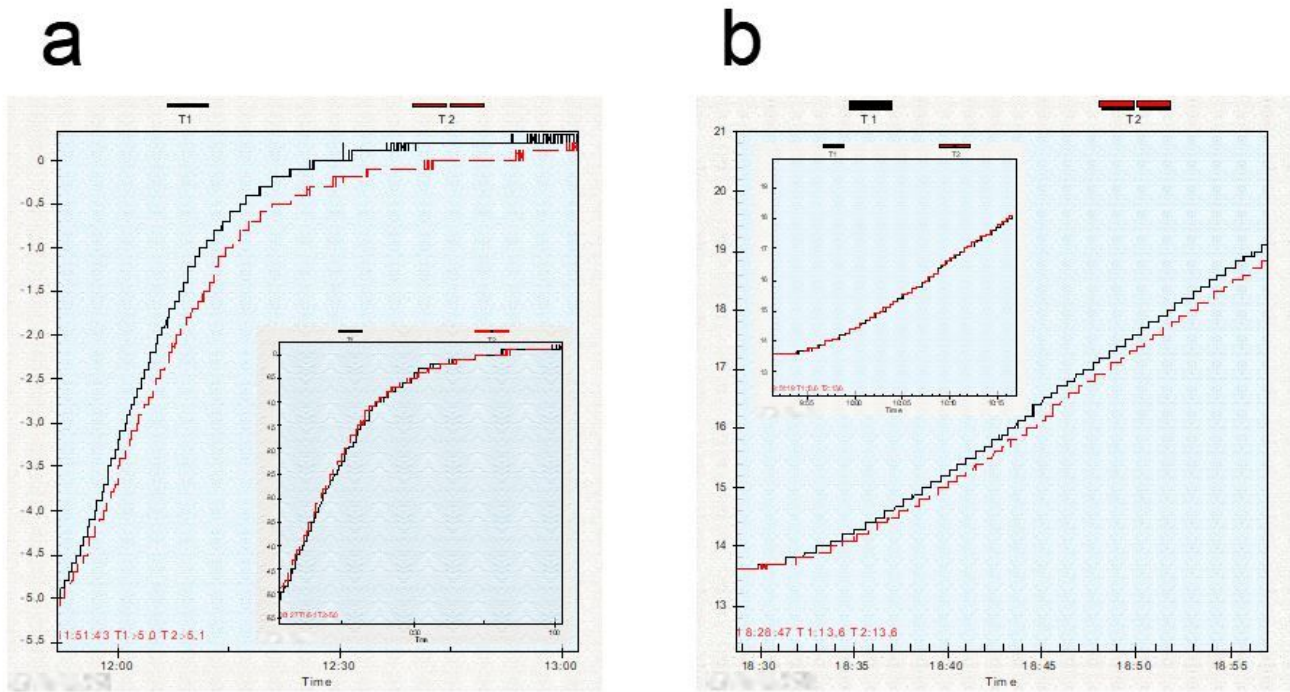


Figure 2

Experimental observation of the transformation UVB into heat by CAT (20 μ M CAThem in 20 mM phosphate buffer pH 7,4, 50 μ M ferrocyanide. Samples of 0,8 ml in silicon sealed PMMA cells of 1x1x1,2mm under UVB intensity 600 μ W/cm². a) Effect of CATUVB on ice melting. Samples were frozen at -19°C and then allowed to melt at 13°C. UVB irradiation started at -5°C. Black line: Temperature recording of CAT sample. Red broken line: temperature recording of control sample. Inset: Temperature recording of two control samples following the same procedure. b) Effect of CATUVB on the temperature of the medium. Samples equilibrated at 13,6 °C were subjected to UVB irradiation until the temperature increased to 19°C. Black and red lines as aforementioned. Inset: Temperature recording of two control samples following the same procedure.

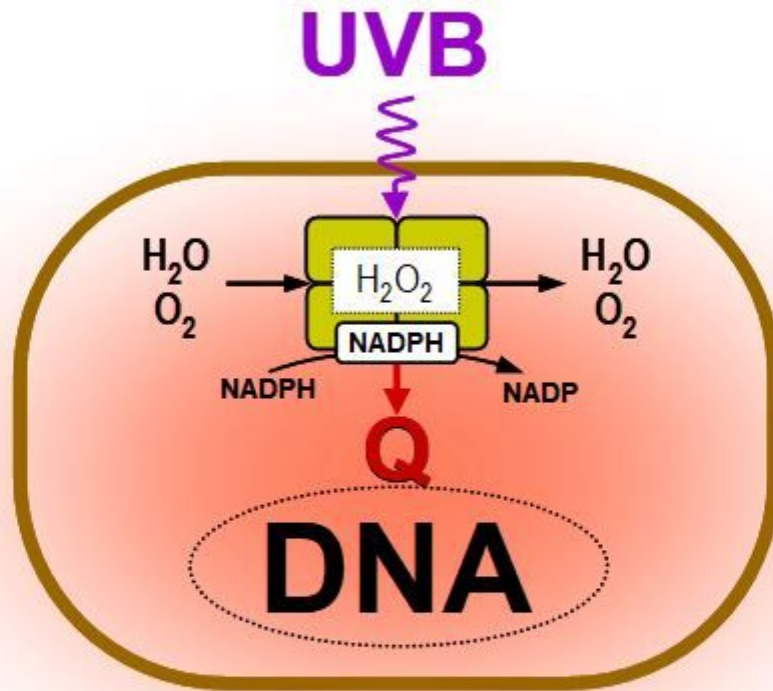


Figure 3

Schematic representation CAT transforming UVB into heat (Q) (red shade) inside a cell. Heat output would be driven by the concentration of NADPH, the oxidation of which by CATUVB inhibits CII formation.

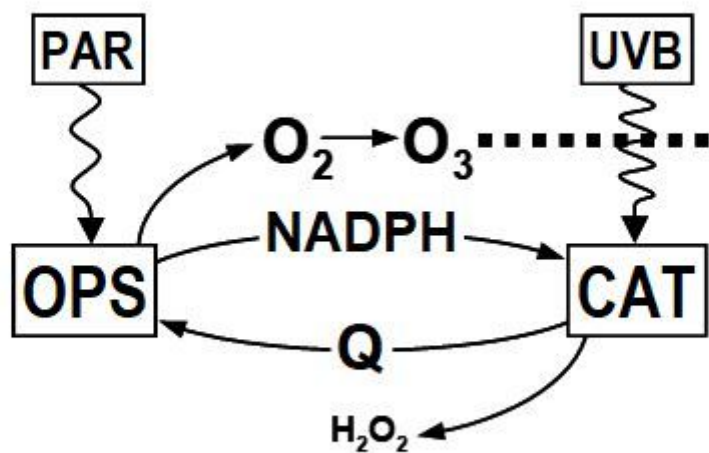


Figure 4

Interactions between CATUVB and oxygenic photosynthesis (OPS). Heat from CATUVB drives OPS, while the products of OPS, NADPH and O_2 , up- and down-regulate CATUVB activity, respectively. H_2O_2 traces are remnants of CATUVB activity (Figure 1c).